

**Cavitation Phenomena and Performance of Oil
Hydraulic Poppet Valve***
(3rd Report, Influence of the Poppet Angle and Oil
Temperature on the Flow Performance)

By Shigeru OSHIMA** and Tsuneo ICHIKAWA***

The influence of the poppet angle and the oil temperature on the flow characteristics and the cavitation phenomena of an oil hydraulic poppet valve are studied experimentally using a half cut model. The following results are obtained. A change of the poppet angle has great effect on the pressure distribution and the flow contraction degree in the restriction between the poppet surface and the valve seat. Hence a remarkable effect of it appears on the valve performances especially when the chamfer is on the seat. The effect of the oil temperature is explained generally by a change in viscosity and Reynolds number.

Key Words : Cavitation, Fluid Power Systems, Poppet Valve, Half Cut Model, Flow Performance, Critical Cavitation Number, Poppet Angle, Oil Temperature, Experimental Study

1. Introduction

A large number of chokes and valves are used in many oil hydraulic systems. When oil flows through the restricted parts such as valves at high velocity, cavitation happens and causes many problems.

Many works have been done concerning the cavitation in the cylindrical chokes, in which the influences of cavitation on the flow characteristics or the effects of dimensions and forms of the chokes on the cavitation performance have been investigated⁽¹⁾. Also the effects of difference of the oil and the chokes materials on the cavitation characteristics have been studied in a recent work⁽²⁾. However, there have been few works concerning the cavitation in the hydraulic valves. Especially, for the poppet valves, authors have never known any studies except for the works by Aoyama et al.⁽³⁾. As the factors which have major effects on the performance of a poppet valve and cavitation phenomenon, the length of chamfer, the poppet angle and the oil temperature are considered. Several experimental results have been reported by Aoyama et al. concerning the effects of the chamfer length and the poppet angle⁽³⁾⁽⁴⁾. There have been, however, few works about the effect of the oil temperature except for the cylindrical chokes⁽¹⁾⁽⁵⁾⁽⁶⁾.

Authors made clear the occurrence process of the cavitation and its effects

* Received 26th March, 1984.

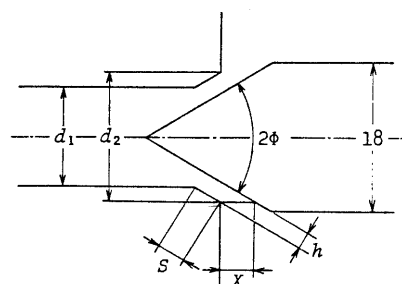
** Lecturer, Numazu College of Technology, (3600 Ooka, Numazu, Shizuoka, Japan)

*** Professor, Toyohashi University of Technology, (1-1 Hibarigaoka, Tenpakucho, Toyohashi, Aichi, Japan)

on the flow performance of a poppet valve as a result of the experimental study using a half cut model in the previous first report⁽⁷⁾. And the influence of the chamfer length on the cavitation characteristics and the flow performance has been investigated in the second report⁽⁸⁾. Now, this third report presents the results of the experimental study concerning the effects of the poppet angle and the oil temperature on the flow performance and the cavitation characteristics of a poppet valve by using the same method as in the previous reports.

2. Method of Experimentation and Arrangement of Results

The test apparatus and the method of



2ϕ	S mm	d_1 mm	d_2 mm	Seat NO.
$90^\circ, 60^\circ, 45^\circ$	0	12.00	—	1
90°	1.32	12.01	13.87	3
60°	0.71	12.03	12.73	5
	1.25	11.99	13.24	6
	2.37	12.01	14.38	7
45°	1.17	11.99	12.88	9

Fig.1 Important dimensions of the test valves

measurements are the same as in the previous reports ⁽⁷⁾⁽⁸⁾. The structure of the half cut model is shown in the first report ⁽⁷⁾. The hydraulic circuit and the definition of the characteristic coefficients used in this paper are given in the second report ⁽⁸⁾.

The important dimensions of the test valves are shown in Fig.1. The vertical angle of the tapered surface of the chamfer is the same as the poppet angle 2ϕ in every case. For the purpose of studying the influence of the poppet angle, the flow characteristics, critical cavitation number, pressure distributions and cavitation noise are measured changing the poppet angle 2ϕ in 90° , 60° and 45° for the both valves with no chamfer and 1.2 mm chamfer on the seat. Valve lift x is set at 0.8 mm, 1.131 mm and 1.478 mm respectively for $2\phi=90^\circ$, 60° and 45° for the purpose of setting the restriction height $h (=x \sin \phi)$ at 0.566 mm in every case. Oil temperature is held at $40 \pm 1^\circ\text{C}$ during the test.

Besides, for the purpose of studying the oil temperature, the same measurements as above are carried out at $\theta=25^\circ\text{C}$, 40°C and 55°C using the valve with $2\phi=60^\circ$ and $S=1.25$ mm. In addition, in order to study the influence of the poppet angle and the chamfer length on the valve performance which depends on the oil temperature change, the discharge coefficients and the critical cavitation numbers are measured at various oil temperatures between 25° and 55°C in both cases of changing 2ϕ with $S=1.2$ mm and changing S with $2\phi=60^\circ$.

The hydraulic oil used here is the same one as used in the previous report. Table 1 shows the density and the viscosity of the oil at each temperature. The critical pressure for air separation is approximately the same as reported by Hibi ⁽⁹⁾.

3. Influence of the Poppet Angle

3.1 Case of the diverging flow

Figure 2 shows the change of the noise level N , discharge coefficient C and the representative pressure P_{**} in the restriction when the downstream pressure P_2 is gradually reduced with the upstream pressure P_1 fixed at 5 MPa(abs.) for three different poppet angles $2\phi=90^\circ$, 60° and 45° . C is shown for $S=0$ mm and $S=1.2$ mm while N and P_{**} are only for $S=1.2$ mm. P_{**} is the pressure at a particular point on the valve seat where the most clear

Table 1 Density and viscosity of the oil

Temperature θ °C	Density ρ Kg/m ³	Viscosity μ Pa.s
25	864	10.1×10^{-2}
30	858	7.55
35	854	5.77
40	851	4.60
45	848	3.59
50	845	2.90
55	841	2.37

pressure reduction appears with an increase of ΔP in the restriction. The pressure $P_{0.2}$ measured at 0.2 mm inside of the restriction from the entrance is plotted in the case of $2\phi=90^\circ$, and $P_{0.4}$ in two other cases. The mark of \blacktriangleright in Fig.2 indicates the cavitation inception, \blacktriangleright and (\blacktriangleright) show the cavitation occurrence at the entrance corner. Incipient cavitation occurs just behind the edge of the restricted part in the case of $S=0$ mm. On the other hand, the cavitation inception occurs far downstream of the restriction and then cavitation appears also at the entrance corner after that in the case of $S=1.2$ mm.

C_c indicated by thin lines in Fig.2 show the discharge coefficients calculated by the following equation with $S=1.2$ mm, and these coefficients indicate the difference of the flow contraction degree among the three cases.

$$C_c = Q / \{a_1(x) \sqrt{2(P_1 - P_{**}) / \rho}\} \quad \dots (1)$$

where Q is the volumetric flow rate, $a_1(x)$ the flow passage area at the entrance of the restriction. Figure 2 shows that C_c is smaller as 2ϕ is larger, which suggests the contraction is stronger in the restriction. This tendency is caused by the difference of the flow bending angle at the entrance corner. The values of C show the same tendency in the case of $S=0$ mm.

It is understood that the contraction of the streamline is weakened by the existence of the chamfer, because C_c is larger than C of $S=0$ mm in the range of no cavitation. This fact is clearer as 2ϕ is smaller. As 2ϕ is larger, C becomes large in spite of the smaller C_c because the pressure falls more sharply just behind the entrance of the restriction.

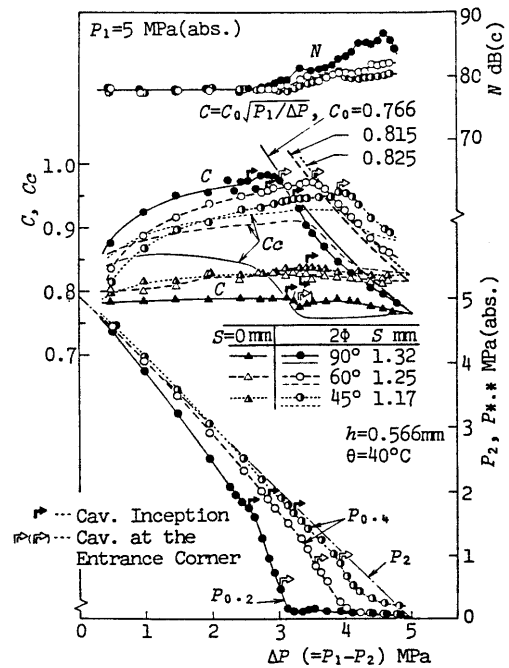


Fig.2 Flow characteristics (diverging flow)

C_c falls sharply with cavitation occurrence at the entrance and becomes equal to C obtained with $S=0$ mm and $P_2=0$ MPa(abs.) in the case of $2\phi=90^\circ$. Namely, it is suggested that the flow separates completely from the seat at the entrance and the contraction degree of stream line is nearly the same as in the case of $S=0$ mm. Even with the cavitating condition, the contraction seems to be weakened since C_c is larger than C of $S=0$ mm when 2ϕ is small. The fact is understood also by comparison of the results obtained by the equation $C=C_v\sqrt{P_1/\Delta P}$ (8) with the measurements in Fig 2. C is smaller as 2ϕ is larger when the cavitation occurs at the entrance, and the tendency is the same as the case of $S=0$ mm.

Cavitation occurs at less ΔP and the saturation of flow rate appears more clearly as 2ϕ is large in the case of $S=1.2$ mm. It is also noticeable that the noise level with $2\phi=90^\circ$ is higher than in the other two cases.

Figure 3 shows the critical cavitation number against the change of Reynolds number Re^* with a constant h and several different values of 2ϕ . Both limits to the inception and the occurrence at the entrance are shown with $2\phi=90^\circ, 60^\circ$ and 45° . The curves above in Fig.3 show the data for $S=0$ mm and the under curves show those for $S=1.2$ mm.

K_c is larger as 2ϕ is larger, but the difference is not so clear in the case of $S=0$ mm. It is considered from the result of the pressure distribution, of which data are not shown here, that there is not so large a difference in the downstream pressure condition that it has great effect on the cavitation inception. Namely, though the difference is clear

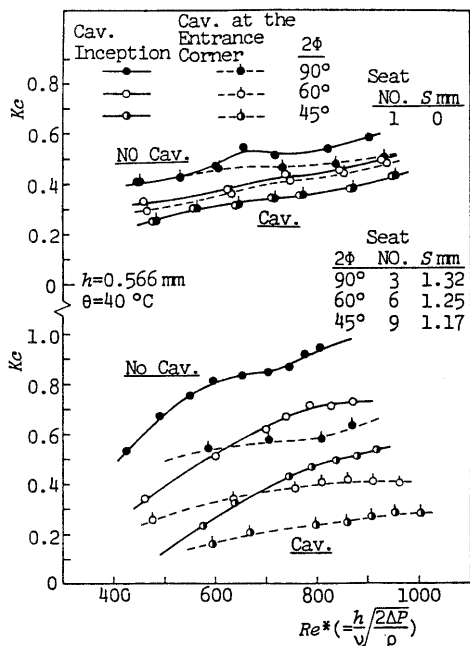


Fig.3 Critical cavitation number (diverging flow)

among the pressure distributions in the upstream region, the pressure is equal to P_2 just behind the restricted part in every case.

On the other hand, both the critical cavitation numbers for the inception and the occurrence at the entrance show a clear tendency to become larger with an increase of 2ϕ in the case of $S=1.2$ mm. Namely, the change of 2ϕ has great effect on the cavitation occurrence when the chamfer is on the seat, because a great difference is produced in the pressure distributions by a change of the corner angle at the entrance and an expanding range of the flow passage in the restriction according to the change of 2ϕ .

The difference between the critical cavitation numbers for the inception and the occurrence at the entrance is small in the range of small Re^* , and it is large as 2ϕ is larger with a fixed Re^* .

Figure 4 shows the pressure distributions measured along the seat surface. Both results under the cavitating and the non-cavitating conditions are indicated. Since the pressure reduction is greater just behind the entrance of the restriction and less great in the upstream region as 2ϕ is larger, the pressure drop gradient is very steep near the entrance of the restriction. On the other hand, since the pressure reduction due to the stream bending at the entrance corner is less, the pressure lowest point moves to the inner part and the pressure reduction becomes greater in the upstream region, the pressure drop gradient is gentle near the entrance of the restriction with a decrease of 2ϕ . These results make clear the effect of 2ϕ on the flow characteristics and the limit to the cavitation occurrence.

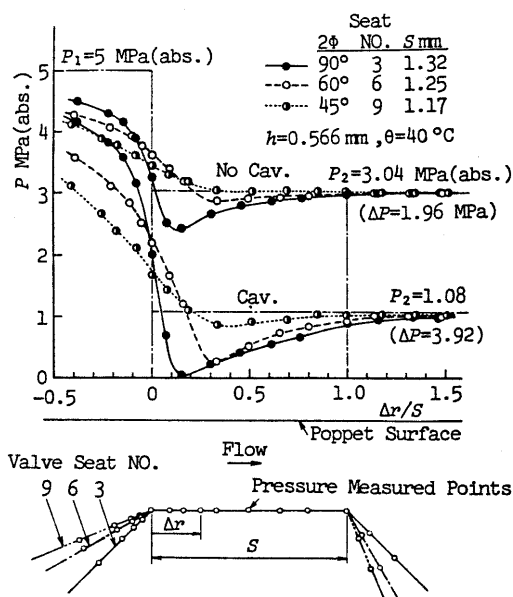


Fig.4 Pressure distribution on the valve seat (diverging flow)

3.2 Case of the converging flow

Figure 5 shows the flow characteristics with reduction of P_2 under the constant $P_1=5$ MPa(abs.) in the case of a converging flow. The symbols used in Fig.5 are the same as in Fig.2, and the mark * indicates the desinence point of cavitation. C_c is calculated by the following equation.

$$C_c = Q / \{a_2(x) \sqrt{2(P_1 - P_{0.1}) / \rho}\} \quad \dots \quad (2)$$

where $a_2(x)$ is the flow passage area at the entrance of the restriction in the case of the converging flow.

The incipient cavitation occurs far downstream of the outlet of the restriction, and then cavitation appears also at the entrance with a more reduction of P_2 in the case of $2\phi=90^\circ$ and $S \pm 1.2$ mm. On the other hand, cavitation inception occurs suddenly at the entrance with a light shock and the pressure falls below the atmospheric pressure in the restriction, the flow rate increases discontinuously and saturates to a constant value in the case of $2\phi=45^\circ$. The same tendency appears in the case of $2\phi=60^\circ$. There is a hysteresis between the inception and the desinence of cavitation. It appears more clearly in the case of $2\phi=45^\circ$. The same phenomenon has been reported in the cylindrical choke (11). We have found that the same discontinuous change happened also in the case of $2\phi=90^\circ$ when S was shorter than in this case.

C_c is larger than C of $S=0$ mm in the range with no cavitation. C_c is larger as 2ϕ is larger in contrast to the case of a

diverging flow. C_c falls discontinuously with cavitation occurrence and becomes equal to C of $S=0$ mm with $P_2=0$ MPa(abs.) in the cases of $2\phi=60^\circ$ and 45° . It suggests that the contraction degree of the stream line is nearly the same as in the case of $S=0$ mm. However, an extreme pressure reduction in the restriction induces a discontinuous increase of C even with a strong contraction.

The discontinuous flow increase appears also in a sharp edged seat valve with $2\phi=60^\circ$ and 45° . There is also a hysteresis between the inception and desinence of cavitation with $2\phi=45^\circ$. Though the data of pressure distribution are not shown here, the discontinuous pressure drop in the range of 0.4 and 0.6 MPa below P_2 happens just behind the restriction on the valve seat side. In the case of small 2ϕ , the poppet surface and the valve seat wall form a narrow expanding clearance between them in the downstream side, in which the choking phenomenon happens partially in the same way as with the chamfered valve. Since the choking is not complete, the flow increases slightly with ΔP .

The noise tends to be greater as 2ϕ is smaller, especially a loud noise including metallic sound happens with cavitation occurrence and severe jet turbulence in the case of $2\phi=45^\circ$.

Figure 6 shows the limit to the cavitation occurrence. K_c is larger as 2ϕ is smaller in contrast to the diverging flow. The difference is not so clear in the case of $S=0$ mm.

In the case of $S \pm 1.2$ mm, there is a large difference between the critical cavitation numbers for the inception and the occurrence at the entrance with $2\phi=90^\circ$, but there is little difference with $2\phi=45^\circ$. The limit to the inception has a

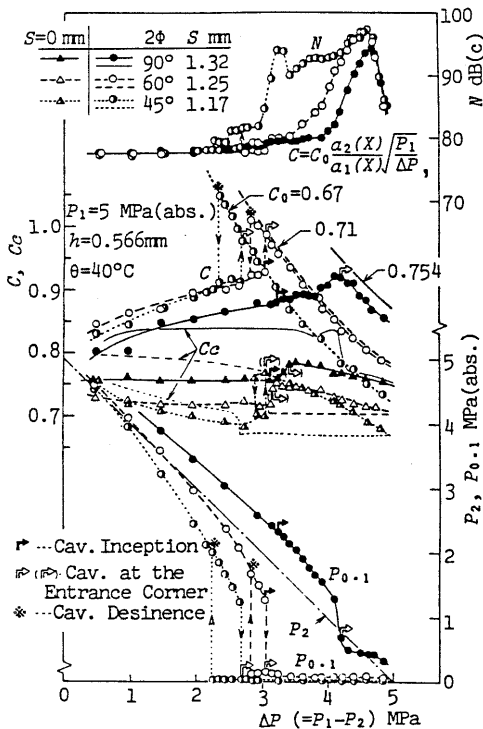


Fig.5 Flow characteristics (converging flow)

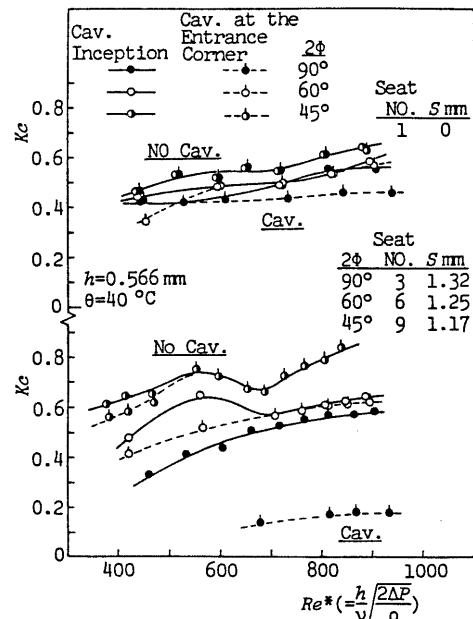


Fig.6 Critical cavitation number (converging flow)

maximum and the difference between the inception and the occurrence at the entrance becomes large between $R_2^*=500$ and 600 in the case of $2\phi=60^\circ$. The difference disappears almost when R_2^* is larger than 700. It is understood that the limit to the cavitation occurrence at the entrance is particularly influenced by a change of 2ϕ in the converging flow.

Figure 7 shows the pressure distributions along the valve seat. As 2ϕ is less, the angle of the flow bending at the entrance corner becomes larger and the expanding degree of the flow passage smaller. Hence the pressure reduction becomes greater just behind the entrance, and the form of the pressure distribution becomes similar to that in the diverging flow. The pressure recovers and becomes approximately P_2 near the outlet of the restriction when the cavitation does not occur. However, when the cavitation occurs at the entrance, the pressure falls below the atmospheric pressure in the restriction and it does not recover easily even in the downstream region especially with $2\phi=60^\circ$ and 45° .

The flow reattaches to the valve seat in the restriction and locally decelerates because of an expanding of the stream line under the no cavitating condition. On the other hand, when cavitation occurs at the entrance and a choking happens, the flow passes the restriction without reattachment and deceleration as the flow is separated completely and the valve seat surface is covered with cavities. Hence, the pressure recovery does not happen. It is considered that a discontinuous change in the flow characteristics is caused by such alteration of the flow pattern.

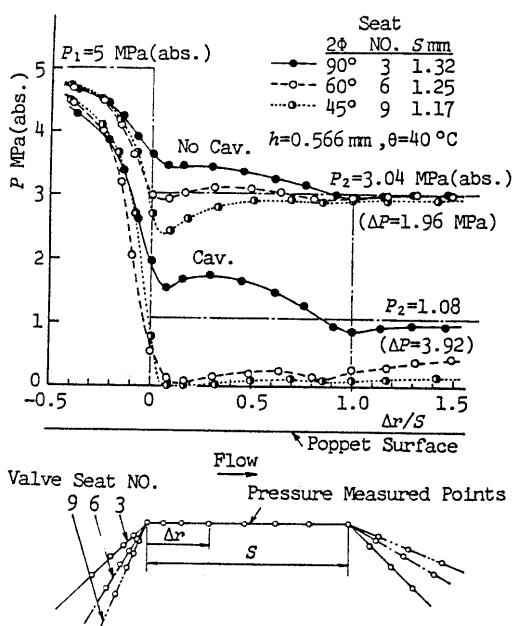


Fig.7 Pressure distribution on the valve seat (converging flow)

4. Effect of Oil Temperature

4.1 Case of the diverging flow

Figure 8 shows the flow characteristics with a change in the oil temperature θ as $25^\circ, 40^\circ$ and 55°C in the case of $2\phi=60^\circ$ and $S=1.25\text{ mm}$. The equation and the calculated curve in Fig.8 are obtained for 40°C and they are the same as in Fig.2.

C is larger as θ is higher in the range with no cavitation, but the difference becomes very little when cavitation occurs at the entrance. The pressure in the restriction $P_{0.4}$ is low as θ is high but there is not so clear a difference.

Comparing the curves of C_c , it is understood that the difference between them is very clear in the range of small values of ΔP but becomes not so clear when ΔP increases. The difference becomes immediately very small when cavitation occurs at the entrance. C_c is the product of the velocity coefficient and the contraction coefficient ⁽¹⁰⁾. It is therefore considered that the difference of C_c depends on the velocity coefficient as the viscosity of oil changes in a wide range with θ in this case. Namely, the effect of viscosity appears greatly on C_c as the flow reattaches to the surface of the seat in the range of small values of ΔP , while it becomes less since the flow separates more completely from the seat with an increase of ΔP . It becomes approximately zero when the cavitation occurs at the entrance because the flow passes the restriction without reattachment such as the flow in the sharp edged orifice.

Figure 9 shows the limits to the cavitation occurrence with a change of the oil temperature for three different values of 2ϕ with $S=1.2\text{ mm}$ and constant $\Delta P=1.96\text{ MPa}$. K_c becomes higher and the difference

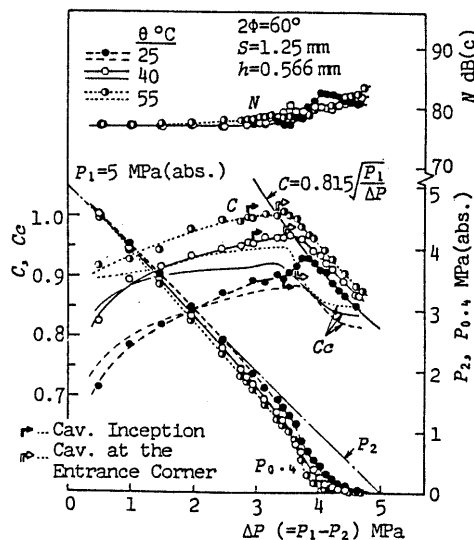


Fig.8 Effect of θ on the flow characteristics (diverging flow)

between the limits to the inception and to the occurrence at the entrance becomes larger with an increase of θ and R_*^* . This fact agrees with the case in Fig.3 of ΔP changing with θ constant.

It is found in Fig.9 that the limit to the inception of $2\phi=90^\circ$ decreases in the range of high R_*^* . Figure 10 shows the measurements of K_c with changing θ and P_1 under the same condition as in Fig.9. K_c for the inception shows a maximum at about $R_*^*=1000$ and decreases immediately to become equal to K_c for the occurrence at the entrance in the range of $R_*^*\geq 1000$. Comparing this with the result in the second report⁽⁶⁾, it is considered that K_c becomes maximum when the flow is unstable at the boundary condition between reattachment and no reattachment in the restriction. In the range of higher R_*^* , cavitation occurs at the entrance in the

incipient stage as the flow separates completely and the flow pattern is similar to that in the sharp edged orifice. Also the result of discharge coefficient in Fig.12 makes clear this fact.

Figure 11 shows the effect of the oil temperature with change of S . The limit to the inception is influenced clearly by θ and R_*^* . On the other hand, the limit to the occurrence at the entrance is not so clearly affected and the value of K_c is approximately equal to that of $S=0$ mm. The limit to the inception becomes maximum for $S=0.71$ mm in the range of little R_*^* and the maximum point moves to larger S with an increase of R_*^* . This tendency agrees with the result obtained with a changing ΔP in the second report.

Figure 12 shows the discharge coefficients with five different values of ΔP and seven values of θ under the no cavitating condition. The curves above in Fig.12 indicate the results measured with three different 2ϕ with $S=1.2$ mm and the

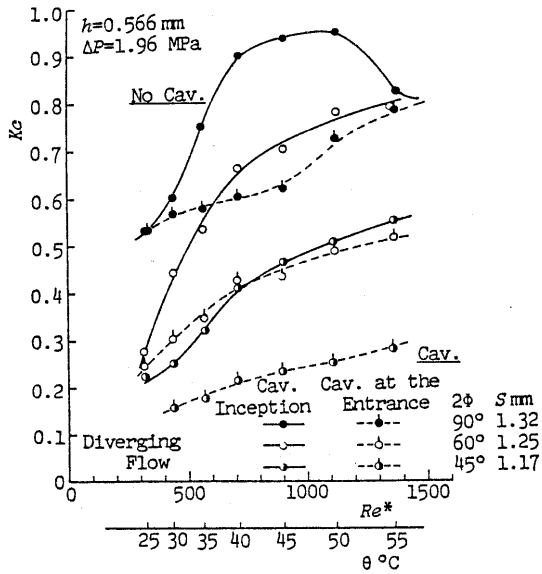


Fig.9 Effect of θ and 2ϕ on the critical cavitation number

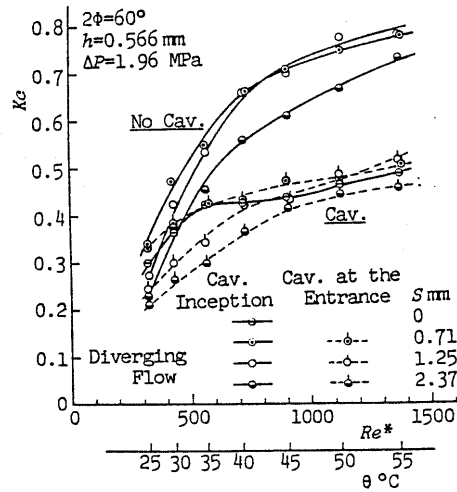


Fig.11 Effect of θ and S on the critical cavitation number

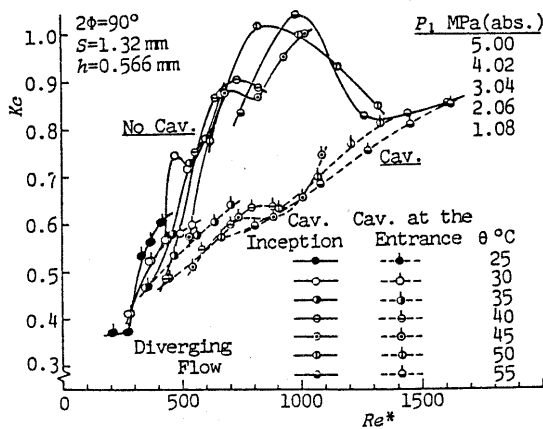


Fig.10 Critical cavitation number with change of P_1 and θ ($2\phi=90^\circ$)

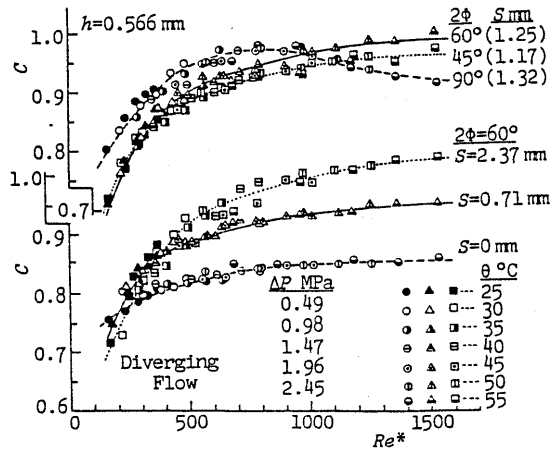


Fig.12 Discharge coefficient with change of θ , 2ϕ and S

curves below the results measured with three different S with $2\phi=60^\circ$.

It is understood that the discharge coefficients are able to be expressed as a function of Re^* independently of θ and ΔP . C is larger as 2ϕ is larger in the range of little Re^* . However, in the case of $2\phi=90^\circ$, C decreases with an increase of Re^* in the range of $Re^*\geq 1000$ in the same manner as the sharp edged orifice. It is also understood that C changes more clearly with θ and Re^* as S is larger.

4.2 Case of the converging flow

Figure 13 shows the effect of θ on the flow characteristics with $2\phi=60^\circ$ and $S=1.25$ mm in the converging flow. The equation and calculated curve of C in Fig.13 are obtained at 40°C and they are the same as those in Fig.5.

The pressure in the restriction $P_{0.1}$ drops more sharply and C becomes larger as θ is higher under no cavitating condition. However, the difference among the three cases becomes approximately zero when cavitation occurs at the entrance of the restriction. The discontinuous change and the hysteresis appear clearly as θ is lower. The hysteresis does not appear at $\theta=55^\circ\text{C}$.

Comparing the curves of C_c , it is understood that C_c increases with ΔP at $\theta=25^\circ\text{C}$ because the effect of viscosity is great, but it decreases at $\theta=55^\circ\text{C}$ because the effect of contraction becomes stronger. When the cavitation occurs and the flow separates completely at the entrance, C_c drops and becomes a constant value at 0.69 in every θ . The discontinuous change of C_c is clear as θ is lower.

Figure 14 shows the performances of N , C and $P_{0.2}$ with an increase of θ at the constant P_1 and P_2 . It shows that the discontinuous change happens also with the

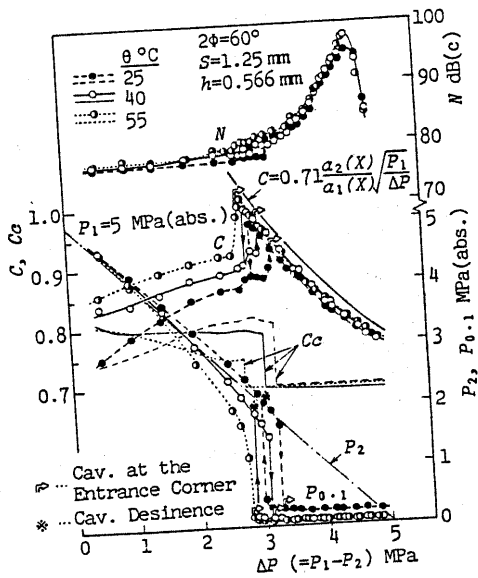


Fig.13 Effect of θ on the flow characteristics (converging flow)

change of θ . It is often experienced in practical hydraulic systems that the cavitation noise and the system pressure fluctuation suddenly happen even under a steady running condition. The same phenomenon in the cylindrical chokes has been reported (5).

Figure 15 shows the effect of the oil temperature on the limit to the cavitation occurrence with three different values of 2ϕ for the constant $\Delta P=1.96$ MPa in the case of $S=1.2$ mm.

Even if Re^* is fixed, there is difference between the results of K_c .

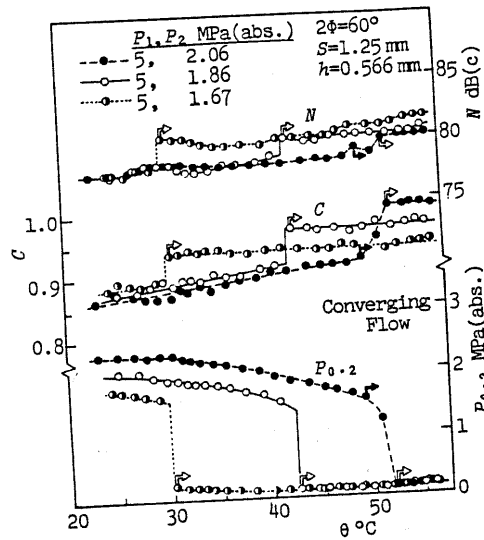


Fig.14 Change of N , C and $P_{0.2}$ with θ

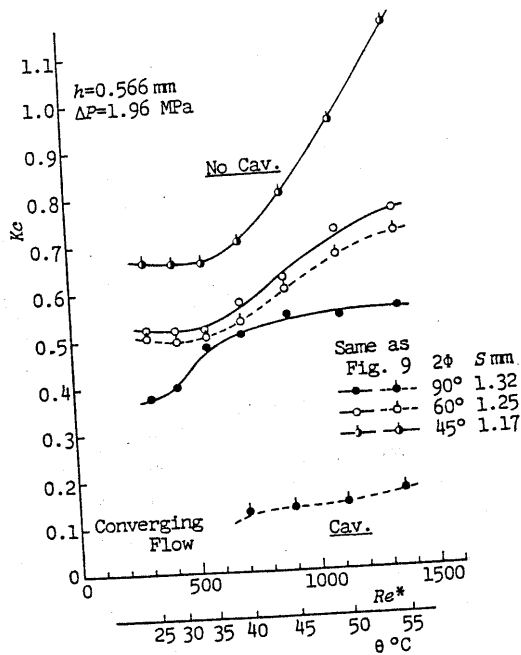


Fig.15 Effect of θ and 2ϕ on the critical cavitation number

measured with changing ΔP and with changing θ . Hence the curves in Fig.16 fairly differ from those in Fig.6. But, the basic tendencies are similar to each other. That is, K_c increases more clearly as 2ϕ is smaller with an increase of θ and Re^* in the range of high Re^* . The tendency is particularly clear at $2\phi=45^\circ$. Figure 16 shows the effect of the oil temperature with the change of S in the case of $2\phi=60^\circ$. The change of K_c is greater in $S=1.25$ mm than in the other cases. The reason is given as follows; the flow reattaches to the seat surface in the restriction within the range of low θ and Re^* but the flow condition approaches the boundary on which a reattachment occurs or not in the restriction with the increase of θ and Re^* , so that K_c increases clearly. In the other cases, the degree of change of K_c is relatively small since the change of the flow pattern as mentioned above does not happen.

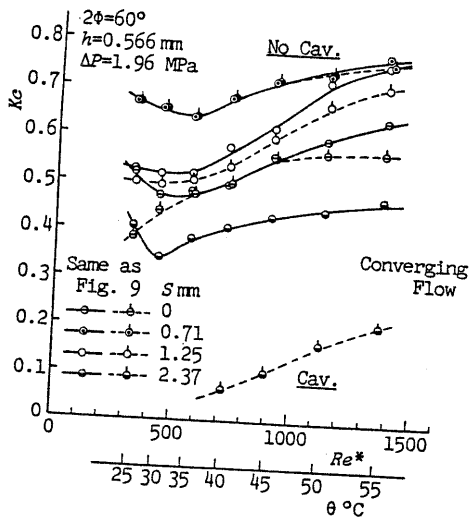


Fig.16 Effect of θ and S on the critical cavitation number

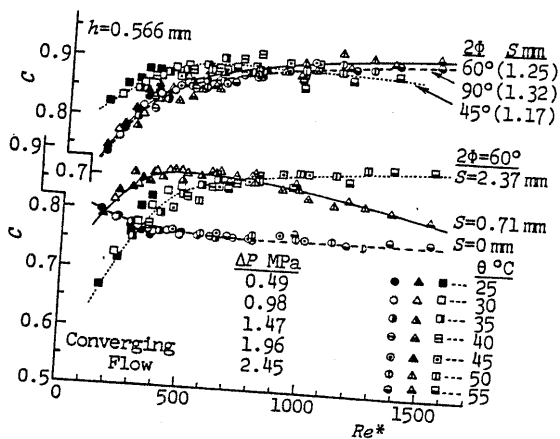


Fig.17 Discharge coefficient with change of θ , 2ϕ and S

Figure 17 shows the discharge coefficients measured with changing ΔP and θ under no cavitating condition. In the case of $2\phi=45^\circ$ with $S=1.17$ mm and $2\phi=60^\circ$ with $S=0.71$ mm, C shows large values within the range of little Re^* because of the pressure reduction in the restriction. However, they show the tendency to decrease with an increase of Re^* because the separation and the contraction become severe in the range of high Re^* .

5. Conclusions

The effects of the poppet angle 2ϕ and the oil temperature θ on the flow characteristics and the cavitation occurrence are studied experimentally by using a half cut model of an oil hydraulic poppet valve. The result makes clear the facts as follows.

The influence of 2ϕ appears clearly in the case of the chamfered seat valves. The change of 2ϕ has great effect on the contraction of flow and the pressure distribution in the restriction, which induces particular changes in the flow and the cavitation characteristics. It is also found that a discontinuous change happens in the flow characteristics with little 2ϕ in the case of a converging flow. The effect of θ greatly depends on the change of viscosity as has been mentioned by Backé et al. (8). Thus the effect of θ can be expressed by the change of Re^* . The discontinuous change in the flow characteristics is induced also by the change of θ with the cavitation occurrence in the case of the converging flow.

The authors wish to thank Mr. Hibi in Toyohashi University of Technology for his useful advice.

References

- (1) Backé, W. and Benning, P., Ind. Anz., Nr. 63 (1962-8), p. 1563.
- (2) Yamaguchi, A. and Saito, H., J. Hy. & Pneu. (in Japanese), Vol. 13, No. 4 (1982-7), p. 53.
- (3) Aoyama, Y., et al., J. Hy. & Pneu. (in Japanese), Vol. 7, No. 2 (1976-3), p. 105.
- (4) Aoyama, Y., et al., Trans. Jpn. Soc. Mech. Eng. (in Japanese), Vol. 49, No. 447, B (1983-11), p. 2282.
- (5) Ichikawa, T., et al., J. Hy. & Pneu. (in Japanese), Vol. 13, No. 6 (1982-9), p. 411.
- (6) Backé, W. and Riedel, H.-P., Ind. Anz., 94, Jg. Nr. 8 (1972-1), p. 153.
- (7) Oshima, S. and Ichikawa, T., Trans. Jpn. Soc. Mech. Eng. (in Japanese), Vol. 51, No. 462, B (1985-2), p. 427.
- (8) Oshima, S. and Ichikawa, T., Trans. Jpn. Soc. Mech. Eng. (in Japanese), Vol. 51, No. 462, B (1985-2), p. 628.
- (9) Hibi, A., J. Hy. & Pneu. (in Japanese), Vol. 4, No. 3 (1973-7), p. 41.
- (10) Kasai, K., Trans. Jpn. Soc. Mech. Eng. (in Japanese), Vol. 33, No. 251 (1967-7), p. 1088.
- (11) Pearce, I. D. and Lichtarowicz, A., Proc. 2nd Fluid Power Sym., D2 (1971-1), p. 13.